Japanese Journal of
Applied Physics

Study on dry etching of epitaxially grown $Si_{0.7}Ge_{0.3}$ and Si using H_2 diluted CF_4 plasma

To cite this article before publication: Kotaro Ozaki *et al* 2025 *Jpn. J. Appl. Phys.* in press https://doi.org/10.35848/1347-4065/adea81

Study on Dry Etching of Epitaxially Grown $Si_{0.7}Ge_{0.3}$ and Si using H_2 Diluted CF_4 Plasma

Kotaro Ozaki[1]*, Yusuke Imai[1], Takayoshi Tsutsumi[2], Yuki Imai[1], Noriharu Takada[2], Kenji Ishikawa[2], Yuji Yamamoto[3,1], Wei-Chen Wen[3] and Katsunori Makihara[1,3]

[1]*Graduate School of Engineering, Nagoya University, Furo-cho, Chikusa-ku, Nagoya 464-8603, Japan*

[2]*Center for Low-Temperature Plasma Sciences, Nagoya University, Furo-cho, Chikusa-ku, Nagoya 464-8603, Japan*

[3]*IHP – Leibniz-Institut für Innovative Mikroelektronik, Im Technologiepark 25, 15236 Frankfurt (Oder), Germany*

E-mail: *ozaki.koutaro.g8@s.mail.nagoya-u.ac.jp

The influence of H_2 dilution on CF_4-plasma etching of $Si_{0.7}Ge_{0.3}$ on Si(001) and Si on $Si_{0.7}Ge_{0.3}$/Si(001) was investigated. Selective etching of $Si_{0.7}Ge_{0.3}$ with respect to Si was achieved without H_2 dilution, with the selectivity ratio of approximately 5.0. As the H_2 dilution ratio increased, the etch rate of $Si_{0.7}Ge_{0.3}$ decreased monotonically, while that of Si remains nearly unchanged up to 5% H_2 dilution and the etch rate decreased by further H_2 dilution. With an increase in the H_2 dilution, fluorocarbon deposition on $Si_{0.7}Ge_{0.3}$ and Si surface increased, resulting in suppression of surface roughening. Note that, the selectivity ratio of approximately 3.5 with keeping a surface flatness was achieved with 5% H_2 dilution. Furthermore, fluorocarbon passivation was more prominent on Si than $Si_{0.7}Ge_{0.3}$. We demonstrated lateral selective etching of $Si_{0.7}Ge_{0.3}$ by etching of the <110>-oriented sidewalls of $Si_{0.7}Ge_{0.3}$/Si/$Si_{0.7}Ge_{0.3}$ stacked layers. These results are applicable to Si-nanosheet fabrication for gate-all-around field-effect transistors.

1. Introduction

Nowadays, gate-all-around field-effect transistors (GAAFETs) are center to the aggressive scaling of silicon complementary metal-oxide-semiconductor (CMOS) technology, in line with Moore's Law, and replacing FinFETs[1-3]. GAAFETs enable device operation with excellent switching characteristics by incorporating multilayer Si-nanosheets (Si-NSs) as the channel in a three-dimensional array, which realize effective current controllability through GAA structures. Therefore, from the perspectives of integration and low power consumption, GAAFETs play a pivotal role in enabling high-performance artificial intelligence accelerators. In other words, the GAAFETs are key features in next-generation chips and promise substantial improvements in power efficiency and processing speeds.[4-5] One of the key processes in forming Si-NSs for GAAFETs is the epitaxial growth of SiGe/Si layer stacks and the selective etching of the SiGe layers. Recently, there have been many reports all over the world as conventional methods for selective etching of SiGe with respect to Si, which mainly include wet etching,[6-11] HCl vapor phase etching,[12-19] and dry etching.[20-23] It should be noted that by precise control of the H_2 dilution ratio in H_2/CF_4, SiGe and Ge selective dry etching with respect to Si can be realized.[24-26] Although these studies provide systematic investigations of dry etching for blanket SiGe or Ge films, fabricating Si-NS devices with reasonable yield from SiGe/Si stacked structures requires precisely controlled lateral selective etching of SiGe from vertically patterned stacks. After the lateral SiGe etching, atomically flat top and bottom Si surfaces are required. Therefore, understanding the surface reactions involved in dry etching is essential for developing etching processes with atomic-level precision.

In this work, we investigate dry etching processes of epitaxially grown SiGe(001) and Si(001) surfaces using a CF_4 and evaluate influence of H_2 dilution of a plasma on the selectivity and surface roughness. Furthermore, the selective etching of SiGe in lateral <110> direction is tested for a Si-NS application using the CF_4 diluted with H_2 plasma.

2. Experimental methods

Selective dry etching of SiGe is carried out using H_2-diluted CF_4 plasma. To investigate the surface reactions involved in selective SiGe etching and to evaluate lateral selectivity, SiGe layers and Si/SiGe stacked layers were fabricated using conventional reduced-pressure chemical vapor deposition (RP-CVD) with a H_2–SiH_4–GeH_4 gas mixture.[27] After wet chemical cleaning steps, a 500 nm-thick SiGe layer with a Ge content of 30% was epitaxially grown at 600°C on the n-Si(001) substrate. We also fabricated a 500 nm-thick Si layer with

buried $Si_{0.7}Ge_{0.3}$ marker layer on the n-Si(001) using the H_2–SiH_4 and H_2–SiH_4–GeH_4 gas system, respectively. To prevent plastic relaxation of the $Si_{0.7}Ge_{0.3}$ marker, the first 50 nm of Si cap was deposited at 600ºC, followed by the growth of 450 nm-thick Si layers at 700ºC. After that, dry etching using H_2 diluted CF_4 plasma was performed, where the total gas flow rate and pressure were kept constant at 100 sccm and 2.0 Pa, respectively. The H_2 dilution ratio was varied from 0% to 15%. The dry etching reactor used in this work is shown in Fig. 1. Process gases are introduced into the reactor through a shower head. The top- and bottom-electrode frequencies were set at 100 MHz and 2 MHz, respectively. Here, input power to the top electrode for the plasma discharge was kept constant at 100 W without any power was applied to the bottom electrode. The substrate was placed on the bottom electrode. To avoid heating the sample during the etching process, substrate temperature was maintained at 20ºC by a back-side cooling with He. The layer thickness after each etching step was evaluated using in-situ spectroscopic ellipsometry (SE). Surface morphology and root-mean-square (RMS) roughness were characterized by atomic force microscopy (AFM) in the tapping mode. In addition, X-ray photoelectron spectroscopy (XPS) was performed to evaluate chemical bonding features at a take-off angle of 30º. Here, a monochromatized Al-Kα line with a photon energy of 1486.6 eV was used as the X-ray source, where the spot size was 500 μm. For a Si-NS fabrication, lateral etching using H_2-diluted CF_4 plasma was performed from $Si_{0.7}Ge_{0.3}$/Si/$Si_{0.7}Ge_{0.3}$ stacked layers. In this experiment, 50 nm-$Si_{0.7}Ge_{0.3}$/50 nm-Si/50 nm-$Si_{0.7}Ge_{0.3}$ layer stacks with 0.1 mm line and space photoresist patterns are used. After that, $Si_{0.7}Ge_{0.3}$/Si/$Si_{0.7}Ge_{0.3}$ line-patterns were formed by vertical etching with the 13% H_2 diluted CF_4 plasma under substrate bias application at 200 W. Subsequently, lateral etching was carried out using the 5% and 10% H_2 diluted CF_4 plasma without bias application in the same chamber, where etching times were set at 10 min and 20 min. Before and after etching, the structures of the $Si_{0.7}Ge_{0.3}$/Si/$Si_{0.7}Ge_{0.3}$ stacked layer were evaluated by scanning electron microscopy (SEM).

3. Results and discussion

Figure 2 shows the etch rates of $Si_{0.7}Ge_{0.3}$ and Si, as evaluated from in-situ SE measurements, as a function of the H_2 dilution ratio. When the samples were exposed to CF_4 plasma without H_2 dilution, the etch rates of $Si_{0.7}Ge_{0.3}$ and Si layer were approximately 0.3 nm/s and 0.06 nm/s, respectively, in which selectivity was 5.0. Considering that the binding energies of Si–Ge (3.12 eV) and Ge–Ge (2.84 eV) bonds are lower than that of Si–Si bonds (3.25 eV),[28] this result suggests that F radicals preferentially cleave Si–Ge and Ge–Ge bonds

over Si–Si bonds. However, the Si-rich layer was hardly detected at the etch front of the $Si_{0.7}Ge_{0.3}$ surface by XPS analysis (not shown). This indicates that surface Si atoms are also etched simultaneously because the bonds between the surface Si atoms and the underlying substrate are weakened due to the preferential removal of Ge atoms via Si–Ge/Ge–Ge bond etching. The etch rate of $Si_{0.7}Ge_{0.3}$ decreases with increasing H_2 dilution, and etching is barely detectable at dilution ratios of 13% or higher. As discussed in ref. 29, F radicals decrease exponentially with an increase of the H_2-dilution ratio. Therefore, this result can be interpreted as a decrease in the probability of etching due to the exponential decrease in F radicals with the addition of H_2. On the other hand, the etch rate of Si is almost unchanged up to 5% of the H_2 dilution ratio. With an increase in the H_2 dilution ratio, the etch rate gradually decreased. As discussed in ref. 30, selective etching of Si over SiGe can be achieved by irradiation with hydrogen plasma, since hydrogen combines with Si more easily than with Ge. Therefore, hydrogen might have contributed slightly to the etching of Si by enhancing the F-radical-induced breaking of Si-Si bonds. Although the total amount of CF_4 gas decreased with the introduction of H_2, the reduction in the etch rate of Si was slower than that of $Si_{0.7}Ge_{0.3}$. By further increasing the H_2-dilution ratio to 13%, the etching of Si was still confirmed, while the etching of $Si_{0.7}Ge_{0.3}$ was hardly detected. Further detailed discussion and research are needed to understand the phenomenon at the H_2-dilution ratio over 13%. As a result, the etching ratio of the $Si_{0.7}Ge_{0.3}$/Si decreases with increasing H_2 dilution ratio, although $Si_{0.7}Ge_{0.3}$ is etched more selectively than Si in the range of H_2-dilution ratio from 0% to 10%.

To evaluate the influence of the H_2 dilution on the surface morphology of $Si_{0.7}Ge_{0.3}$ and Si, we measured topographic images using an AFM. As shown in Fig. 3, the $Si_{0.7}Ge_{0.3}$ and the Si surfaces before dry etching were smooth with RMS roughness of approximately 0.12 nm, and 0.11 nm, respectively. However, after dry etching using the CF_4 plasma without H_2 dilution, the RMS roughness increased to approximately 0.81 nm for $Si_{0.7}Ge_{0.3}$, and 0.66 nm for Si. It is interesting to note that, after etching using the H_2 diluted CF_4 plasma at dilution ratio of 5% and 10%, the RMS roughness of both $Si_{0.7}Ge_{0.3}$, and Si surfaces decreased to approximately 0.30 nm, as summarized in Fig. 4, which indicates uniform etching with suppressed surface roughness is achieved by introducing the H_2 gas. This result might be attributable to the fact that the decrease in F radicals may have increased the amount of deposited fluorocarbon, which acted as a protective layer and suppressed surface reactions. Note that we also confirmed that there was no significant change in the surface RMS roughness of the samples before and after wet cleaning steps to remove a surface

fluorocarbon (not shown).

To clarify the difference in chemical bonding features of the surface after the CF_4 plasma etching with and without H_2 dilution, C 1s core-line spectra were measured as shown in Fig. 5. Note that the peak intensities were normalized by the Si 2p metallic spectrum based on the Ge content of Si and $Si_{0.7}Ge_{0.3}$ layers, and binding energies were calibrated by the C 1s spectrum. For the as-deposited samples and those taken after etching with CF_4 plasma, signals in the range from 286 eV to 295 eV were hardly detected, although signals due to absorption of hydrocarbon were observed at 285 eV. When the samples were etched using CF_4 plasma diluted with H_2 at 5%, signals attributed to the C_x–F_y bonds[31-32] were observed, which indicated that fluorocarbon was deposited on the sample surface. The peak intensities of fluorocarbon increase with increasing H_2 dilution ratio. This result can be interpreted in terms of an increase in the amount of fluorocarbon with an increase in the H_2 dilution ratio. As summarized in Fig. 6, the integrated signal intensities corresponding to C_x–F_y bonds exhibit an exponentially increase. According to ref. 29, the concentration of F radicals decreases exponentially with an increase in H_2 dilution. Therefore, this result can be reasonably attributed to the similar underlying mechanisms as those reported in previous research work. Therefore, these results suggest that, at the H_2 dilution ratio over 13%, fluorocarbon deposition becomes a rate-limiting factor for etching. It should be noted that the integrated signal intensity of the fluorocarbon on the Si surface is larger than that on the $Si_{0.7}Ge_{0.3}$ surface. This result implies that the amount of deposited fluorocarbon on the Si surface is more than the $Si_{0.7}Ge_{0.3}$ surface because, from considering to thermal equilibrium conditions,[25] Si–C phases are more stable than Ge–C phases. In addition, it can also be seen that there are mainly four components in the C 1s spectra, except for the signal from the substrate, which is originating from C–CF_2, CF, CF_2, and CF_3 bonds.[25,31,32]

Based on these results, the surface reaction of $Si_{0.7}Ge_{0.3}$ and Si, and the impact of H_2 dilution, can be interpreted under different conditions depending on the dilution ratio as follows: Without any H_2 dilution, the CF_4-plasma etching of $Si_{0.7}Ge_{0.3}$ is more pronounced than that of Si because the Si–Ge and Ge–Ge bonds have lower binding energy than the Si–Si bonds. With an increase in the dilution ratio to 5%, the etch rate of $Si_{0.7}Ge_{0.3}$ is still higher than that of Si. Here, the etching of $Si_{0.7}Ge_{0.3}$ and Si by F radicals decreases since F combines with H to form HF and the amount of F radicals decreases by H_2 introduction. Therefore, the etch rate of $Si_{0.7}Ge_{0.3}$ reduced. However, the etch rate of Si is almost unchanged due to the assistance of hydrogen. On the other hand, a reduction of F radicals causes an increase in the deposited fluorocarbon. Namely, in addition to the reduction of F radicals, passivation by

fluorocarbon on the surface is also a factor that suppresses etching. However, the selective etching of $Si_{0.7}Ge_{0.3}$ is maintained although the selectivity ratio of $Si_{0.7}Ge_{0.3}$ to Si decreases to approximately 3.5. In addition, when the dilution ratio is increased over 5%, the rates of $Si_{0.7}Ge_{0.3}$ and Si further decrease while keeping the selective etching of $Si_{0.7}Ge_{0.3}$. This can be explained that the etching of Si is more suppressed than $Si_{0.7}Ge_{0.3}$ because fluorocarbon deposits on Si more than $Si_{0.7}Ge_{0.3}$ although hydrogen slightly acts as an etchant on Si. It is interesting noted that the selectivity is reversed at a H_2 dilution ratio of 13%. With further increases in the dilution ratio up to 15%, the etching of $Si_{0.7}Ge_{0.3}$ and Si hardly occurred. Namely, the fluorocarbon deposition might be a dominant factor for suppression of the etching by using CF_4 gas at H_2-dilution ratios over 13%.

To demonstrate lateral selective etching of $Si_{0.7}Ge_{0.3}$ with respect to Si, lateral etching was performed after the vertical etching using CF_4 plasma diluted with H_2, as shown in Fig. 7. After etching with the 13% H_2 diluted CF_4 plasma under substrate bias application at 200 W, we can see the vertical anisotropic etching of the $Si_{0.7}Ge_{0.3}$/Si/$Si_{0.7}Ge_{0.3}$ stacked layers, as shown in Fig. 7(a). As discussed in Figs. 5 and 6, fluorocarbons are expected to deposit on the sidewalls of the $Si_{0.7}Ge_{0.3}$/Si/$Si_{0.7}Ge_{0.3}$ stacked layers during anisotropic etching, acting as a protective layer. Subsequent etching using the 10% H_2 diluted CF_4 plasma without bias application, selective etching of the $Si_{0.7}Ge_{0.3}$ layers to lateral direction was confirmed, as shown in Figs. 7(b, b'). However, the etch rate is lower than in the vertical etching experiments. This result might be attributable to the <110> crystal orientation of the sidewalls, in contrast to the (001) orientation and a conformally deposited fluorocarbon causing a limiting factor due to the decrease in ions impact of the lateral etching. On the other hand, when the H_2-dilution ratio is decreased to 5%, we can clearly see the formation of the approximately 113 nm-width Si-NS due to selective etching of the $Si_{0.7}Ge_{0.3}$ layers even for 10 min, as shown in Figs. 7(c), which means that the etch rate of the $Si_{0.7}Ge_{0.3}$ layers is faster than the case of the H_2 dilution of 10%. This result implies that the etching was promoted due to an increase in F radicals with decreasing H_2 dilution, even in lateral etching. With an increase in the etching time to 20 min, it was found that the Si-NS became more significantly triangular shape than the case for 10 min although the selective etching of the $Si_{0.7}Ge_{0.3}$ progressed in which sheet-width in the lateral direction increased from approximately 113 nm to 136 nm. This result can be interpreted as follows: After the etching of the $Si_{0.7}Ge_{0.3}$ layers, the top and bottom surfaces of the Si layer are exposed, and subsequent etching of Si-NS proceeds slightly from both the top and bottom sides, while fluorocarbon remains deposited on the sidewalls.

4. Conclusion

We found that by controlling the H_2 dilution ratio, the selective etching of $Si_{0.7}Ge_{0.3}$ with respect to Si can be achieved while maintaining uniform etching and surface flatness, with the RMS roughness as low as 0.30 nm due to fluorocarbon deposition. Furthermore, by using H_2 diluted CF_4 plasma, we demonstrated selective lateral etching of $Si_{0.7}Ge_{0.3}$ layers and the subsequent formation of Si-NSs from $Si_{0.7}Ge_{0.3}$/Si/$Si_{0.7}Ge_{0.3}$ stacked structures.

Acknowledgments

This work was supported in part by the Fund for the Promotion of Joint Intentional Research [Fostering Joint International Research (A)] 18KK0409 of MEXT Japan. The authors sincerely appreciate the staff of the Center for Low-Temperature Plasma Sciences for their excellent support and Prof. Masaru Hori for his fruitful discussion.

References

1) G. E. Moore, IEEE Solid-State Circuits Newsl. **11**, 33 (2006).
2) M. M. Waldrop, Nature **530**, 144 (2016).
3) R. R. Das, T. R. Rajalekshmi and A. James, IEEE Access **12**, 50556 (2024).
4) D. Jang, D. Yakimets, G. Eneman, P. Schuddinck, M. G. Bardon, P. Raghavan, A. Spessot, D. Verkest and A. Mocuta, IEEE Trans. Electron Devices **64**, 2707 (2017).
5) S. Mukesh and J. Zhang, Electronics **11**, 3589 (2022).
6) G. K. Chang, T. K. Carns, S. S. Rhee and K. L. Wang, J. Electrochem. Soc. **138**, 202 (1991).
7) U. Wieser, D. Iamundo, U. Kunze, T. Hackbarth and U. König, Semicond. Sci. Technol. **15**, 862 (2000).
8) B. Holländer, D. Buca, S. Mantl and J. M. Hartmann, J. Electrochem. Soc. **157**, H643 (2010).
9) V. Loup, L. Gabette, M. -C. Roure, R. Kachtouli, M. Jourdan, P. Besson and S. Petitdidier, ECS Trans. **58**, 47 (2013).
10) K. Komori, J. Rip, Y. Yoshida, K. Wostyn, F. Sebaai, W. D. Liu, Y. C. Lee, R. Sekiguchi, H. Mertens, A. Hikavyy, F. Holsteyns, and N. Horiguchi, Solid State Phenomena **282**, 107 (2018).
11) Z. Baraissov, A. Pacco, S. Koneti, G. Bisht, F. Panciera, F. Holsteyns and U. Mirsaidov, ACS Appl. Mater. Interfaces **11**, 36839 (2019).

12) Y. Bogumilowicz, J. M. Hartmann, R. Truche, Y. Campidelli, G. Rolland and T. Billon, Semicond. Sci. Technol. **20**, 127 (2005).

13) Y. Bogumilowicz, J. M. Hartmann, J. M. Fabri, T. Billon, Semicond. Sci. Technol. **21**, 1668 (2006).

14) V. Destefanis, J. M. Hartmann, S. Borel and D. Bensahel, Semicond. Sci. Technol. **23**, 105019 (2008).

15) Y. Yamamoto, K. Köpke and B. Tillack, Thin Solid Films **517**, 90 (2008).

16) N. Loubet, T. Kormann, G. Chabanne, S. Denorme and D. Dutartre, Thin Solid Films **517**, 93 (2008).

17) Y. Yamamoto, K. Köpke, R. Kurps and B. Tillack, Appl. Surf. Sci. **254**, 6037 (2008).

18) J. M. Hartmann, V. Destefanis, G. Rabillé and S. Monfray, Semicond. Sci. Technol. **25**, 105009 (2010).

19) J. M. Hartmann, B. Previtali, F. Aussenac, P. Dezest, O. Glorieux, A. Blot-Saby, L. Couture and S. Barraud, ECS Trans. **114**, 55 (2024).

20) G. S. Oehrlein, Y. Zhang, G. M. W. Kroesen, E. de Frésart and T. D. Bestwick, Appl. Phys. Lett. **58**, 2252 (1991).

21) G. S. Oehrlein, G. M. W. Kroesen, E. de Frésart, Y. Zhang and T. D. Bestwick, J. Vac. Sci. Technol. **A 9**, 768 (1991).

22) Y. Zhang, G. S. Oehrlein, E. de Frésart and J. W. Corbett, J. Vac. Sci. Technol. **A 11**, 2492 (1993).

23) E. Liu, J. Li, N. Zhou, R. Chen, H. Shao, J. Gao, Q. Zhang, Z. Kong, H. Lin, C. Zhang, P. Lai, C. Yang, Y. Liu, G. Wang, C. Zhao, T. Yang. H. Yin, J. Li, J. Luo and W. Wang, Nanomaterials **13**, 2127 (2023).

24) C. F. Ahles, J. Y. Choi, S. Wolf and A. C. Kummel, ACS Appl. Mater. Interfaces **9**, 20947 (2017).

25) S. W. Robey, A. A. Bright, G. S. Oehrlein, S. S. Iyer and S. L. Delage, J. Vac. Sci. Technol. B **6**, 1650 (1988).

26) A. A. Bright, S. S. Iyer, S. W. Robey and S. L. Delage, Appl. Phys. Lett. **53**, 2328 (1988).

27) J. M. Hartmann, V. Loup, G. Rolland, P. Holliger, F. Laugier, C. Vannuffel and M. N. Séméria, J. Cryst. Growth **236**, 10 (2002).

28) W. M. Haynes, *Handbook of Chemistry and Physics* (CRC Press, Boca Raton, FL, 2016) 97th ed., p. 6-145.

29) M. J. Kushner, J. Appl. Phys. **53**, 2923 (1982).

30) Y. Ishii, R. Scott-McCabe, A. Yu, K. Okuma, K. Maeda, J. Sebastian and J. Manos, Jpn. J.

Appl. Phys. **57**, 06JC04 (2018).

31) C. F. Moffitt, Q. S. Yu, C. M. Reddy, D. M. Wieliczka and H. K. Yasuda, Plasma and Polymers **6**, 193 (2001).

32) T. Nobuta and T. Ogawa, J. Mater. Sci. **44**, 1800 (2009).

Figures

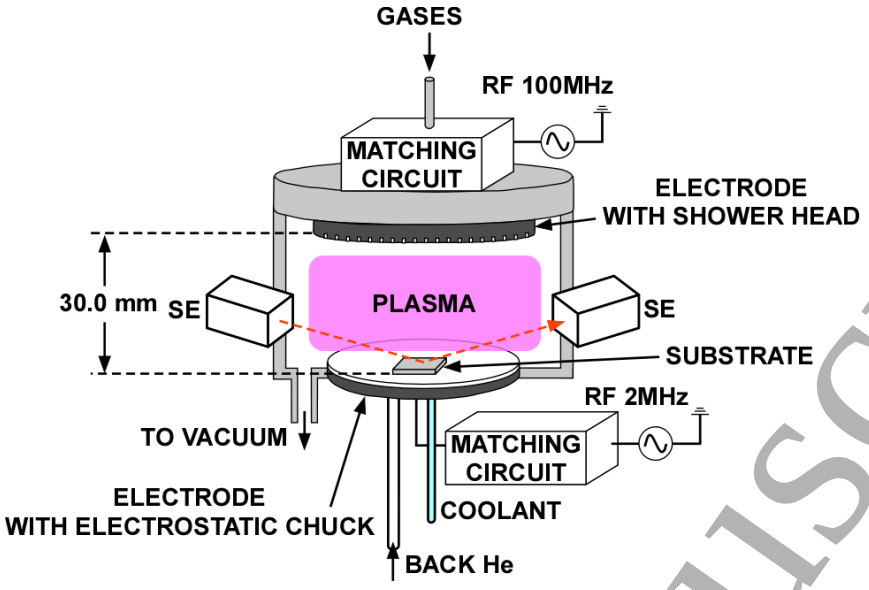

Fig. 1 Schematic illustration of plasma etching reactor used for this work.

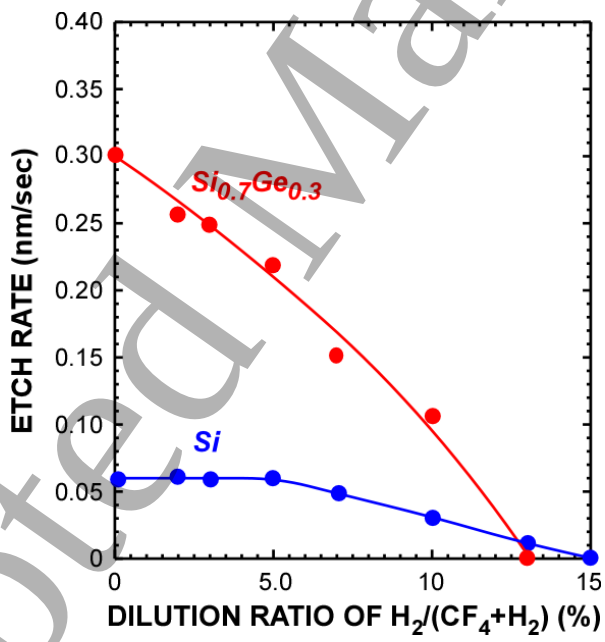

Fig. 2 Etch rates of $Si_{0.7}Ge_{0.3}$ and Si layers as a function of H_2 dilution ratio.

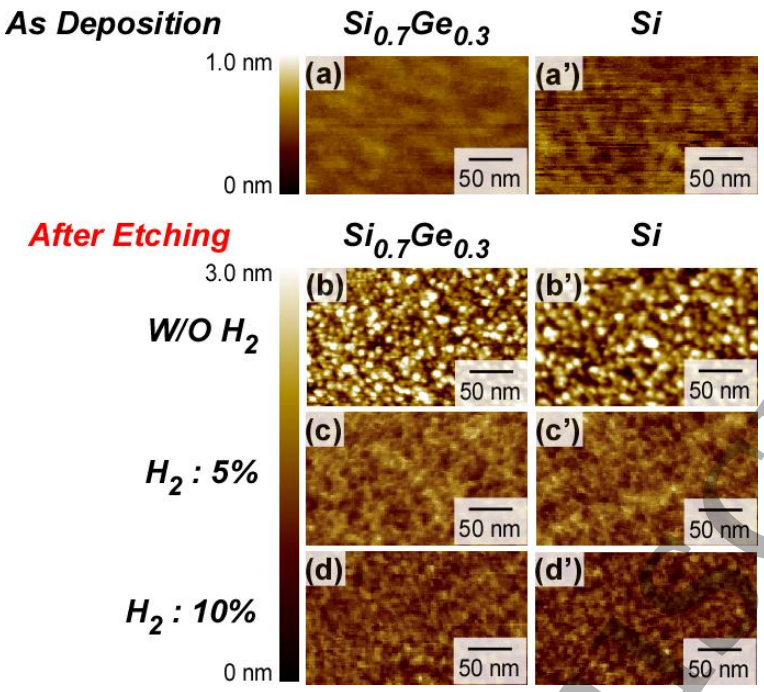

Fig. 3 AFM topographic images of (a, b, c, d) the $Si_{0.7}Ge_{0.3}$ and (a', b', c', d') the Si surfaces taken (a, a') before and after etching using the (b, b') 0%, (c, c') 5% and (d, d') 10% H_2 diluted CF_4 plasma.

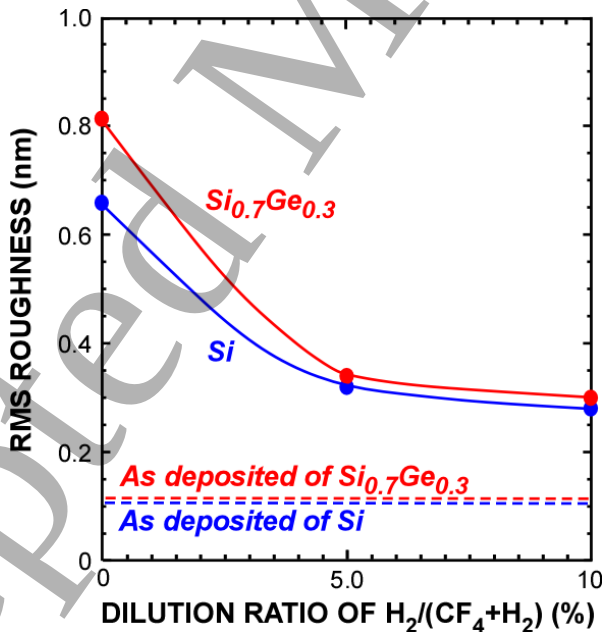

Fig. 4 RMS roughness of the $Si_{0.7}Ge_{0.3}$ and the Si surfaces after dry etching as a function of H_2 dilution ratio. The dry etching time is 1 min.

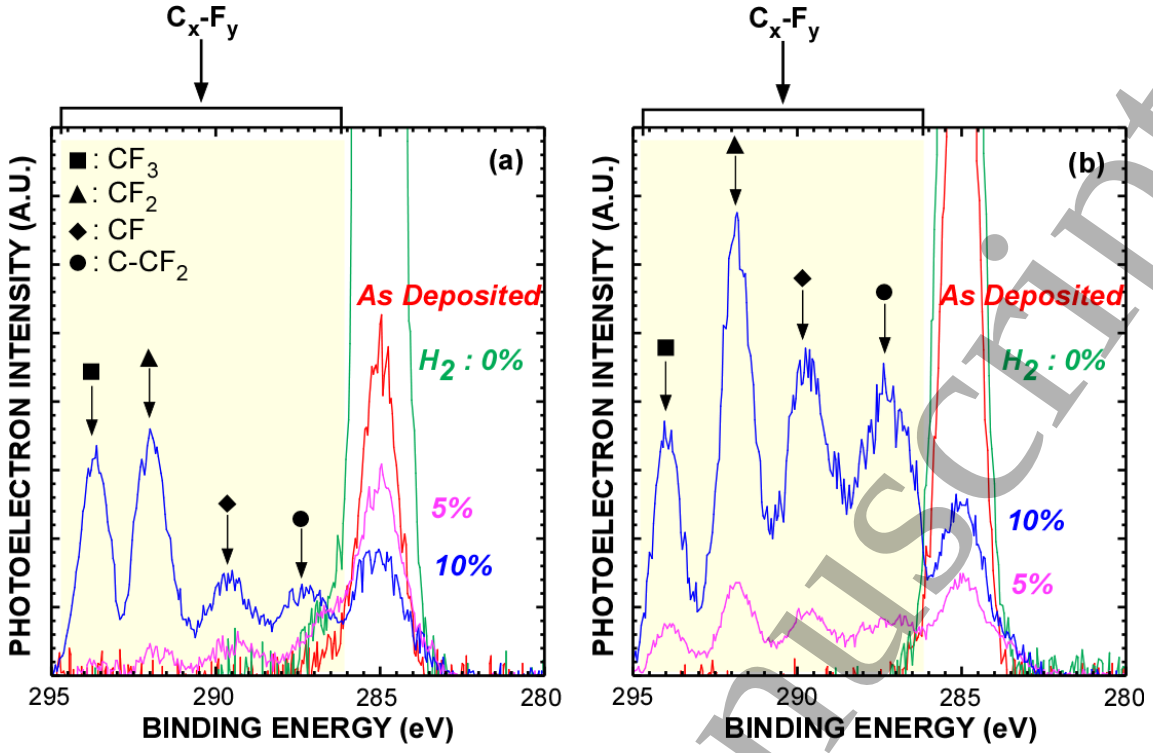

Fig. 5 XPS C 1s core-line spectra of (a) the $Si_{0.7}Ge_{0.3}$ and (b) the Si surface before and after etching using the CF_4 plasma with and without H_2 dilution. In each spectrum, peak intensities were normalized by the Si 2p metallic spectrum, and binding energies were calibrated by the C 1s spectrum.

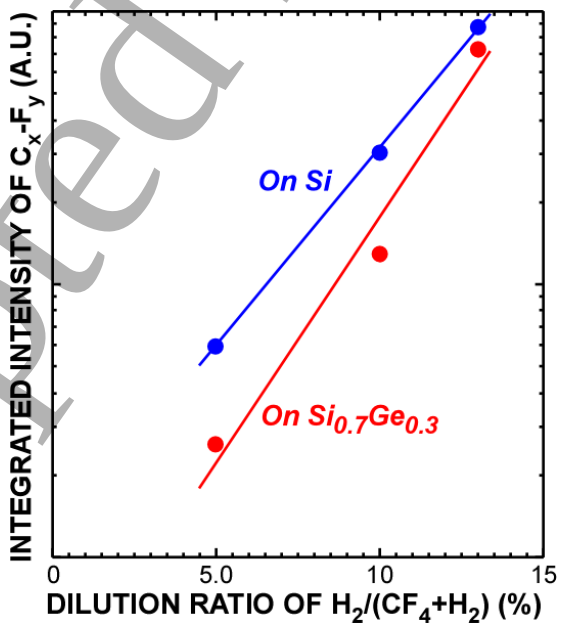

Fig. 6 Integrated area intensities of the C_x–F_y bonds on the $Si_{0.7}Ge_{0.3}$ and the Si surface evaluated from XPS C 1s spectra as a function of H_2 dilution ratio.

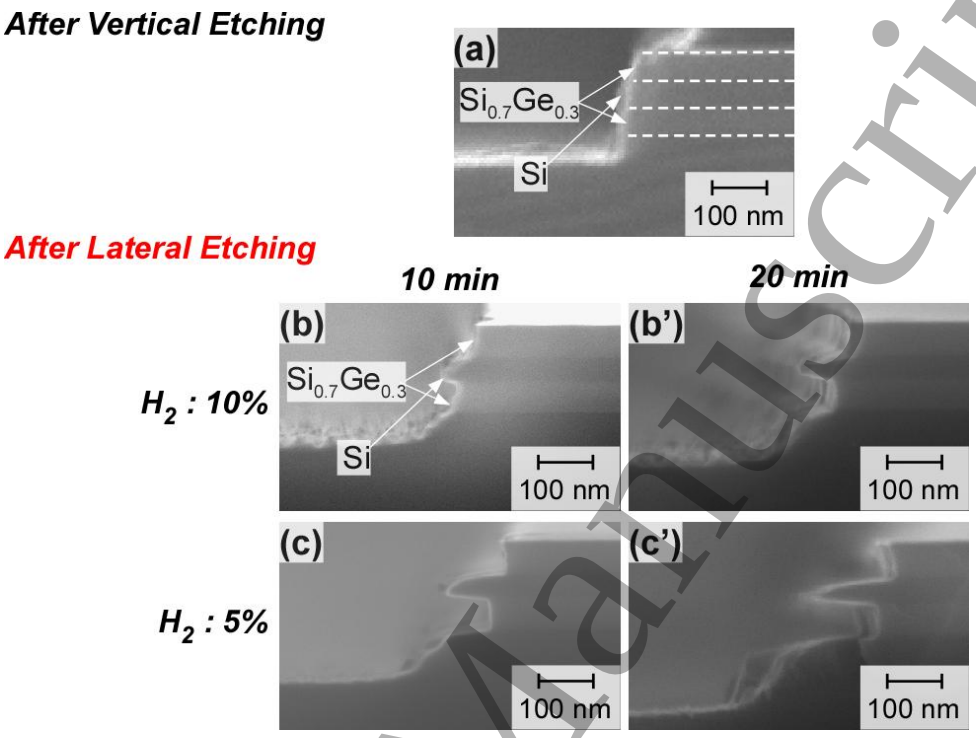

Fig. 7 Cross-sectional SEM images taken after (a) vertical etching using the 13% H_2 diluted CF_4 plasma with the bias application at 200 W, and subsequent lateral etching using the (b, b') 10%, and (c, c') 5% H_2 diluted CF_4 plasma for (b, c) 10, and (b', c') 20 min without bias application.